Randolph et al. (1973) and is presented in Figure 2 of Part I. Now define $\overline{R}[1 + K_c(1 - i)]$ to be R', where R' is composed of system parameters. Therefore, Randolph et al. (1973) have already solved this case too. In fact, if R' is less than equal to R_s where R_s lies on the stability boundary line, then stability is guaranteed:

$$R' \leq R_s \qquad \text{(A23)}$$

or

$$R[1 + K_c(1 - i)] \leq R_s \qquad \text{(A24)}$$

Rearranging Equation (A24) we get the minimum K_c required for stability:

$$K_c \geq (1 - R_s/\overline{R})/(i - 1) \qquad (23)$$

Manuscript received December 6, 1976; revision received April 22, and accepted April 27, 1977.

Predicting the Combustion Rate of Pulverized Fuel from Its Initial Size Distribution

M. E. LEESLEY

Department of Chemical Engineering
University of Texas
Austin, Texas 78712

It is assumed that for pulverized fuel, the weight fraction W with a size larger than x can be expressed as $W = \exp(-bx^n)$. This paper describes the theoretical development and experimental evaluation using pulverized anthracite burning at 30 lb/hr of a method of predicting the combustion rate of a pulverized fuel from the constants b and n in the above equation.

SCOPE

This work was carried out to determine the effect of the initial particle size distribution of a pulverized fuel on its subsequent combustion rate.

With such a relationship available, it was felt that the designers of pulverized fuel firing equipment would be able to calculate the flame parameters that would result from a proposed comminution system. Before the work was undertaken, a substantial amount of data were available relating flame parameters to coal composition, coal-air ratios, flame turbulence and swirl, and combustion temperature and pressure, but nothing was known of the effect of size. Most workers had been deterred by the difficulties of obtaining sized fractions of coal in amounts large enough to sustain a large industrial flame for sufficient time to carry out the necessary measurements.

This work was made possible by the use of high throughput continuous sieving machines to provide the sized fractions and the one-dimensional experimental combustion technique developed by Beer and Thring (1961) which allows the stabilization of a flame with fuel feeds as low as 30 lb/hr.

CONCLUSIONS AND SIGNIFICANCE

The pulverized anthracite and twelve specially sized fractions made from it were burned individually in the experimental furnace. In all, 160 data points were collected. An attempt to correlate the results with conventional relationships for pulverized fuel combustion failed. The data appeared to be related by two separate expressions depending on whether polydisperse or monodisperse fractions of the fuel was burned.

A theoretical approach from basic concepts showed that both of the expressions were special cases of a general expression which was theoretically derived in the course of this work. The general expression could be written solely in terms of the initial particle size distribution of the raw, unsized fuel.

Both sets of experimental data showed good correlation when fitted to the new expression.

A designer of pulverized fuel burning systems is presented with a new tool. Experimental work must still be carried out to find the relationship between combustion

temperature, oxygen concentration, and the combustion rate. The results can be correlated with the equation presented herein, and the designer will be able to vary in advance the initial size parameters to predict the best pulverization method to meet the particular requirements of each design attempted.

Earlier work at the University of Sheffield, England, was carried out into the effect of particle size distribution on the combustion rate of pulverized anthracite. Closely sized fractions of anthracite particles were prepared by sieving from the raw pulverized fuel, and these were burnt in the one-dimensional furnace developed by Beer and Thring (1961).

Because of difficulties encountered when the experimental data were correlated to traditional theory, it was necessary to derive a relationship between the combustion rate, the instantaneous amount of unburnt fuel, and the initial particle size distribution parameters. The following section discusses the argument leading to the development of such a relationship.

THEORETICAL

The Variation of Size Distribution in a Coal Dust Cloud Flame

Let us assume that the initial size distribution of a cloud of particles is defined by the equation

$$W_i = \theta(x) \tag{1}$$

where W_i is the initial fraction by weight of the cloud which consists of particles whose diameter is greater than or equal to x. It will be assumed also that x must lie in the range $x_1 \leq x \leq x_2$, so that whatever the form of the function θ, it must satisfy $\theta(x_1) = 1$ and $\theta(x_2) = 0$.

Differentiation of Equation (1) gives

$$-dW_i = \frac{-d[\theta(x)]}{dx} \cdot dx = \psi(x) \cdot dx$$

where $-dW_i$ is the initial fraction by weight with diameter between x and $x + dx$.

Therefore, the initial mass flow rate of particles with diameter between x and $x + dx$ is $-\dot{m}_o \cdot dW_i$. The initial number flow rate of particles with diameter between x and $x + dx$ is thus given by

$$\frac{-\dot{m}_o \cdot dW_i}{\left(\frac{\pi\rho x^3}{6}\right)}$$

where ρ is assumed to remain constant. The above function implicitly assumes that the particles are spherical in shape.

Let us assume that the diameter of a particle with initial diameter x has been reduced to x_t after the particle has been burning in the flame for a time t. The mass flow rate of the fraction of the cloud under consideration has been reduced to

$$\frac{-\dot{m}_o \cdot dW_i}{\left(\frac{\pi\rho x^3}{6}\right)}\left(\frac{\pi\rho x_t^3}{6}\right)$$

$$= -\dot{m}_o \cdot \frac{x_t^3}{x^3} \cdot dW_i$$

The total mass flow rate of the cloud at time t is therefore

$$\dot{m} = \int^{x=x_2} -\dot{m}_o \cdot \frac{x_t^3}{x^3} \cdot dW_i$$

where the lower limits of integration must be chosen so as to include all initial values of x for which $x_t \geq 0$.

Suppose an initial diameter y_o is defined so that all particles with initial diameter $x \leq y_o$ would have burnt away completely at time t if they had been present in the cloud. The integral for the total mass flow rate at time t can then be written as

$$\frac{\dot{m}}{\dot{m}_o} = \int_{x=z}^{x=x_2} \frac{x_t^3}{x^3}\psi(x)dx \tag{2}$$

where

$$z = x_1 \quad \text{if} \quad y_o \leq x_1$$

and

$$z = y_o \quad \text{if} \quad y_o > x_1$$

In order to determine x_t and y_o, the combustion rate equation for a single particle must be employed. This equation can be written in the form

$$\frac{dm}{dt} = -kf(p_{O_2}, T)D^\beta \tag{3}$$

where m is the mass of a particle with diameter D at time t and k is some numerical constant. Equation (3) can be rewritten in the form

$$\frac{d}{dt}\left(\frac{\pi\rho D^3}{6}\right) = kf(p_{O_2}, T)D^\beta$$

$$\therefore D^{2-\beta}dD \cdot = \frac{-2k}{\pi\rho}f(p_{O_2}, T)dt$$

This integrates to give

$$x^{3-\beta} - x_t^{3-\beta} = \frac{2k}{\pi\rho}(3-\beta)\int_{t=0}^{t=t} f(p_{O_2}, T)dt$$

Letting

$$\phi(t) = \frac{2k}{\pi\rho}(3-\beta)\int_{t=0}^{t=t} f(p_{O_2}, T)dt$$

and

$$q = \frac{1}{3-\beta}$$

we get

$$x^{1/q} - x_t^{1/q} = \phi(t) \tag{4}$$

y_o can be found from Equation (4) as the value of x for which $x_t = 0$; that is

$$y_o^{1/q} = \phi(t) \tag{5}$$

Combining Equations (4) and (5), we get

$$x_t = (x^{1/q} - y_o^{1/q})^q \tag{6}$$

Thus, substituting for x_t in Equation (2), we get

$$\frac{\dot{m}}{\dot{m}_o} = \int_{x=z}^{x=x_2} \frac{(x^{1/q} - y_o^{1/q})^{3q}}{x^3}\psi(x)dx \tag{7}$$

If we let $\bar{x}_i$ be some particle diameter characteristic of the initial distribution and if we define the dimensionless quantities $X = x/\bar{x}_i$ and $Y = y_o/\bar{x}_i$, Equation (7) becomes

$$\frac{\dot{m}}{\dot{m}_o} = \bar{x}_i \int_Z^{X_2} \frac{(X^{1/q} - Y^{1/q})^{3q}}{X^3} \psi(\bar{x}_i \cdot X)\, dX \qquad (8)$$

where

$$Z = z/\bar{x}_i$$

The lower limit of integration in Equation (8) is given by $Z = X_1$ if $Y \leq X_1$ and $Z = Y$ if $Y > X_1$.

The behavior of the whole cloud can be found by investigating $d\dot{m}/dt$:

$$\frac{d\dot{m}}{dt} = \frac{d\dot{m}}{dY} \cdot \frac{dY}{dt} = \frac{d\dot{m}}{dY} \cdot \frac{d}{dt}\left(\frac{y_o}{\bar{x}_i}\right) = \frac{1}{\bar{x}_i} \frac{d\dot{m}}{dY} \cdot \frac{dy_o}{dt}$$

Now, from Equation (5)

$$y_o = [\phi(t)]^q$$

$$\therefore \frac{dy_o}{dt} = q[\phi(t)]^{q-1} \frac{d}{dt}[\phi(t)]$$

But,

$$\phi(t) = \frac{2k}{\pi\rho q} \int_{t=0}^{t=t} f(p_{O_2}, T)\, dt$$

$$\therefore \frac{d}{dt}[\phi(t)] = \frac{2k}{\pi\rho q} f(p_{O_2}, T)$$

$$\therefore \frac{d\dot{m}}{dt} = \frac{1}{\bar{x}_i} \frac{d\dot{m}}{dY} q[\phi(t)]^{q-1} \frac{2k}{\pi\rho q} \cdot f(p_{O_2}, T)$$

$$= \frac{2k}{\pi\rho\bar{x}_i} (y_o)^{1-1/q} f(p_{O_2}, T) \frac{d\dot{m}}{dy}$$

or

$$\frac{d\dot{m}}{dt} = \frac{2k}{\pi\rho(\bar{x}_i)^{1/q}} f(p_{O_2}, T) Y^{1-1/q} \frac{d\dot{m}}{dY}$$

This can be written in terms of $\dot{m}/\dot{m}_o$ as

$$\frac{d}{dt}\left(\frac{\dot{m}}{\dot{m}_o}\right) = \frac{2k}{\pi\rho(\bar{x}_i)^{1/q}} \cdot f(p_{O_2}, T) Y^{1-1/q} \frac{d}{dY}\left(\frac{\dot{m}}{\dot{m}_o}\right) \qquad (9)$$

$\frac{d}{dY}\left(\frac{\dot{m}}{\dot{m}_o}\right)$ can be found using the mathematical result

$$\frac{d}{dY}\left[\int_a^b g(X, Y)\, dX\right] = \int_a^b \frac{\partial g}{dY}(X, Y)\, dX + g(b, Y)\frac{db}{dY} - g(a, Y)\frac{da}{dY}$$

Applying this result to the differentiation of Equation (9), we get

$$\frac{d}{dY}\left(\frac{\dot{m}}{\dot{m}_o}\right) = \bar{x}_i \frac{d}{dY}\left[\int_{X=Z}^{X=X_2} \frac{(X^{1/q} - Y^{1/q})^{3q}}{X^3}\right] \psi(\bar{x}_i \cdot X)\, dX$$

$$= \bar{x}_i \int_{X=Z}^{X=X_2} -3q \frac{(X^{1/q} - Y^{1/q})^{3q-1}}{X^3} \frac{1}{q} \cdot Y^{1/q-1} \psi(\bar{x}_i \cdot X)\, dX$$

$$= -3\bar{x}_i Y^{1/q-1} \int_{X=Z}^{X=X_2} \frac{(X^{1/q} - Y^{1/q})^{3q-1}}{X^3} \psi(\bar{x}_i \cdot X)\, dX$$

or

$$Y^{1-1/q} \frac{d}{dY}\left(\frac{\dot{m}}{\dot{m}_o}\right) = -3\bar{x}_i \int_{X=Z}^{X=X_2} \frac{(X^{1/q} - Y^{1/q})^{3q-1}}{X^3} \psi(\bar{x}_i \cdot X)\, dX \qquad (10)$$

Substituting into Equation (9), we get

$$\frac{d}{dt}\left(\frac{\dot{m}}{\dot{m}_o}\right) = \frac{-6k}{\pi\rho(\bar{x}_i)^{1/q-1}} f(p_{O_2}, T) \times \int_{X=Z}^{X=X_2} \frac{(X^{1/q} - Y^{1/q})^{3q-1}}{X^3} \psi(\bar{x}_i \cdot X)\, dX \qquad (11)$$

For any given initial size distribution, the integral in Equation (11) is a function solely of Y. Similarly, Equation (8) can be used for any initial size distribution to give $\dot{m}/\dot{m}_o$ in terms of Y only. Combination of Equations (8) and (11) gives the integral in Equation (11) solely in terms of $\dot{m}/\dot{m}_o$ if q and the initial size distribution are specified.

The Form of the Initial Size Distribution Function

It is assumed that the original pulverized material before sieving into limited size range fractions is described by a Rosin-Rammler (1933) distribution:

$$W = \exp(-bx^n) \qquad (12)$$

If the original material is then sieved and only particles with diameters in the range $x_1 \leq x \leq x_2$ are retained, then the size distribution of the sieved material is

$$W_i = \frac{\exp(-bx^n) - \exp(-bx^n_2)}{\exp(-bx^n_1) - \exp(-bx^n_2)} \qquad (13)$$

$$\therefore \psi(x) = \frac{-dW_i}{dx} = \frac{bnx^{n-1}\exp(-bx^n)}{\exp(-bx^n_1) - \exp(-bx^n_2)} \qquad (14)$$

For convenience, $\bar{x}_i$ is defined as

$$\bar{x}_i = \int_{x=0}^{x=\infty} -x \cdot dW \qquad (15)$$

by substituting for W from Equation (12) and integrating

$$\bar{x}_i = \int_0^\infty bnx^n \exp(-bx^n)\, dx \qquad (16)$$

This integral can be evaluated by making the substitution $u = bx^n$ in Equation (16):

$$x_i = \frac{1}{b^{1/n}} \int_{u=0}^{u=\infty} u^{1/n} - \exp(-u)\, du = \frac{\Gamma\left(\frac{1}{n} + 1\right)}{b^{1/n}} \qquad (17)$$

Now, from Equation (14)

$$\psi(\bar{x}_i \cdot X) = \frac{bn(\bar{x}_i \cdot X)^{n-1} \exp[-b(\bar{x}_i \cdot X)^n]}{\exp[-b(\bar{x}_i \cdot X_1)^n] - \exp[-b(\bar{x}_i \cdot X_2)^n]}$$

This expression can be simplified by putting

$$b(\bar{x}_i)^n = b\left[\frac{\Gamma\left(\frac{1}{n} + 1\right)}{b^{1/n}}\right]^n = \left[\Gamma\left(\frac{1}{n} + 1\right)\right]^n = \gamma$$

$$\therefore \psi(\bar{x}_i \cdot X) = \frac{n\gamma}{\bar{x}_i} \frac{X^{n-1}\exp(-\gamma X^n)}{\exp(-\gamma X_1^n) - \exp(-\gamma X_2^n)} \qquad (18)$$

Substitution of this expression into Equations (8) and (9) gives the final forms

$$\frac{\dot{m}}{\dot{m}_o} = \frac{n\gamma}{\exp(-\gamma X_1^n) - \exp(-\gamma X_2^n)} \times \int_Z^{X_2} (X^{1/q} - Y^{1/q})^{3q} X^{n-4} \exp(-\gamma X^n) dX \quad (19)$$

and

$$\frac{d}{dt}\left(\frac{\dot{m}}{\dot{m}_o}\right) = \frac{-6kn\gamma f(p_{O_2}, T)}{\pi\rho(\bar{x}_i)^{1/q}\{\exp(-\gamma X_1^n) - \exp(-\gamma X_2^n)\}} \times \int_Z^{X_2} (X^{1/q} - Y^{1/q})^{3q-1} X^{n-4} \exp(-\gamma X^n) dX \quad (20)$$

The Combustion Rate Equation

Beér and Thring (1961) derived the following combustion rate equations:

$$\frac{\rho\bar{x}_i}{6} \frac{1}{\dot{m}_o^{1/3}\dot{m}^{2/3}} \frac{d\dot{m}}{dt} = k'f(p_{O_2}, T) \quad (21)$$

$$\frac{\rho\bar{x}_i^2}{6} \frac{1}{\dot{m}_o^{2/3}\dot{m}^{1/3}} \frac{d\dot{m}}{dt} = k'f(p_{O_2}, T) \quad (22)$$

Equation (21) was derived assuming that the overall combustion rate was controlled by the rate of chemical reaction at the particle surface. Equation (22) was derived assuming the combustion rate controlling mechanism was the rate of diffusion of oxygen to the particle surface through the film of products surrounding the particle. Both equations were derived assuming that the particle size of the cloud was uniform. These two equations may be rewritten as

$$\frac{\rho\bar{x}_i}{6}\left(\frac{\dot{m}}{\dot{m}_o}\right)^{-2/3} \frac{d}{dt}\left(\frac{\dot{m}}{\dot{m}_o}\right) = k'f(p_{O_2}, T) \quad (23)$$

and

$$\frac{\rho\bar{x}_i^2}{6}\left(\frac{\dot{m}}{\dot{m}_o}\right)^{-1/3} \frac{d}{dt}\left(\frac{\dot{m}}{m_o}\right) = k'f(p_{O_2}, T) \quad (24)$$

Equations (23) and (24) may then be rewritten in the general form:

$$\frac{\pi\rho(x_i)^a}{2k_i}\left(\frac{\dot{m}}{\dot{m}_o}\right)^{-k_2} \frac{d}{dt}\left(\frac{\dot{m}}{m_o}\right) = -kf(p_{O_2}, T) \quad (25)$$

where for chemical control:

$$a = 1; \quad k_1 = 3; \quad k_2 = 2/3; \quad k = -k'\pi$$

and for diffusion control:

$$a = 2; \quad k_1 = 3; \quad k_2 = 1/3; \quad k = -k'\pi$$

It is possible to recalculate the values of k_1 and k_2 by the substitution of Equations (19) and (20) into Equations (25).

Substituting the value of $d/dt\ (\dot{m}/\dot{m}_o)$ from Equation (20) into Equation (25), we get

$$\frac{\pi\rho(\bar{x}_i)^a}{2k_1}\left(\frac{\dot{m}}{\dot{m}_o}\right)^{k_2} \left[\frac{-6kn\gamma \cdot f(p_{O_2}, T)}{\pi\rho(\bar{x}_i)^{1/q}\{\exp(-\gamma X_i^n) - \exp(-X_2^n)\}}\right] \int_Z^{X_2} (X^{1/q} - Y^{1/q})^{3q-1} X^{n-4} \exp(-\gamma X^n) dX = kf(p_{O_2}, T) \quad (26)$$

Rearranging, we get

$$\frac{3n\gamma}{[\exp(-\gamma X_1^n) - \exp(-\gamma X_2^n)]} \cdot \int_Z^{X_2} (X^{1/q} - Y^{1/q})^{3q-1} X^{n-4} \exp(-\gamma X^n) dX = (\bar{x}_i)^{1/q-a} k_1 \left(\frac{\dot{m}}{\dot{m}_o}\right)^{k_2}$$

Thus, setting

$$F(Y) = \frac{3n\gamma}{\exp(-\gamma X_1^n) - \exp(-\gamma X_2^n)} \int_Z^{X_2} (X^{1/q} - Y^{1/q})^{3q-1} X^{n-4} \exp(-\gamma X^n) dX \quad (27)$$

we have

$$F(Y) = k_1\left(\frac{\dot{m}}{\dot{m}_o}\right)^{k_2} \quad (28)$$

EXPERIMENTAL WORK

Introduction

In a recent survey of early work on pulverized coal combustion (Hedley and Leesley, 1965), it was shown that two different combustion rate controlling mechanisms could be involved. These were mass transfer of the oxidant to the surface of the coal particle, referred to as diffusion control, and chemical kinetics at the particle surface, or chemical control.

The masking effects of flame aerodynamics and the large size range of pulverized coal dust clouds hinder experimental determinations to discover which of the above mechanisms is the rate controlling mechanism, under any particular set of conditions. Beér (1961) developed a one-dimensional flame technique in which the important chemical reaction characteristics could be studied without the complex aerodynamic disturbances caused by recirculation found in the conventional enclosed flame.

This paper describes a series of experiments in which dust clouds, first of varying size distributions and second of varying uniform size, were burnt using the Beér technique and the collected data compared with theoretical predictions for a combustion rate controlled by chemical control and diffusion control.

Preparing the Fuel

Over 5 000 kg of South Wales anthracite were pulverized to a size specification of 80% through British Stan-

TABLE 1. SIZE SPECIFICATION OF THE COALS

Coal No.	Mesh sizes*		Size range, μ†
1	Raw pulverized coal		0-200.0
2	−B.S. 110		0-129.0
3	−B.S. 160		0-97.7
4	−B.S. 200		0-76.2
5	−B.S. 250		0-61.0
6	−B.S. 325		0-43.2
7	−B.S. 400		0-33.0
8	−B.S. 325	+B.S. 400	33.0-43.2
9	−B.S. 250	+B.S. 325	43.2-61.0
10	−B.S. 200	+B.S. 250	61.0-76.2
11	−B.S. 160	+B.S. 200	76.2-97.7
12	−B.S. 110	+B.S. 160	97.7-129.0
13	−B.S. 90	+B.S. 110	129.0-160.0

* All meshes were made of phosphor-bronze with the exception of British Standard 400, which was of nylon.
† All sizes are those specified by the mesh manufacturers (Russel Constructions Ltd., London, England).

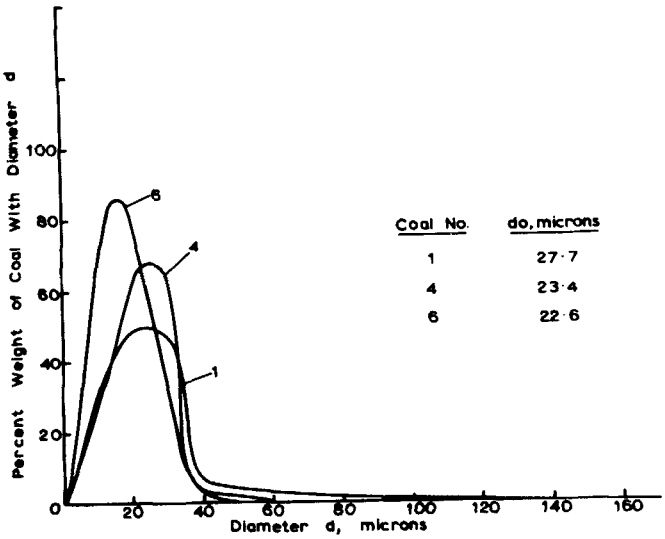

Fig. 1. Size distributions of coals 1, 4, and 6.

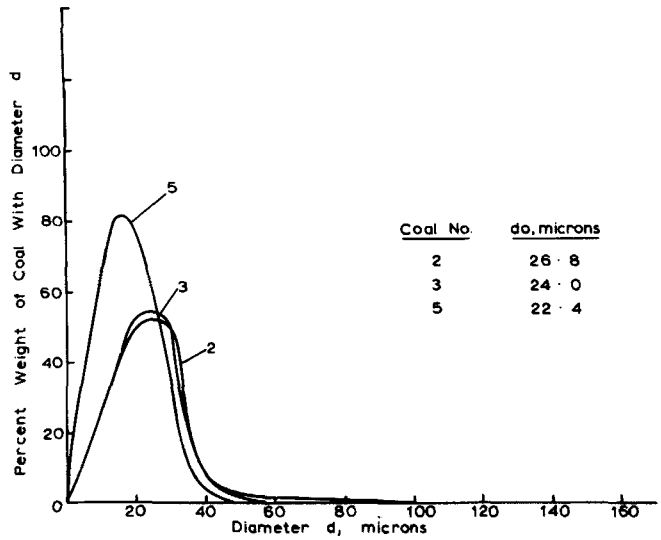

Fig. 2. Size distributions of coals 2, 3, and 5.

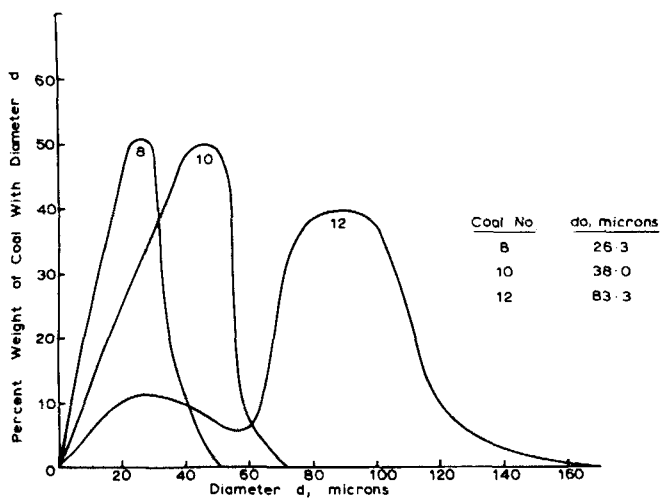

Fig. 3. Size distributions of coals 8, 10, and 12.

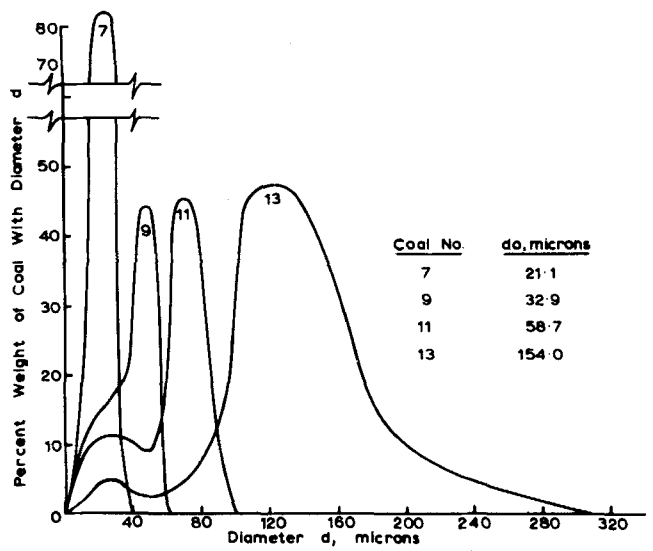

Fig. 4. Size distributions of coals 7, 9, 11, and 13.

dard 200 mesh. Two continuous sieving machines running in series were used to size the coal into two kinds of fractions. Those which were composed of uniformly sized particles are referred to from now on as monodisperse fractions, and those which had a fairly wide size distribution but had a varying amount of the larger sizes removed are referred to as polydisperse fractions.

Table 1 shows the size specifications and the numbering system of the sized fractions produced in this way, and Figures 1 to 4 show the size distribution of each.

Equations (19), (27), and (28) will later be used as the basis for calculating k_1 and k_2. It must be stressed at this point, however, that the form of the equations are such that that k_1 and k_2 are dependent on the Rosin-Rammler constants b and n, only.

The Experimental Runs

The coal fractions listed in Table 1 were burnt in the one-dimensional flame under approximately stoichiometric conditions and at a rate of 14 kg/hr (30 lb/hr). The furnace was a refractory cylinder 6 m long, and of 450 mm diameter, with probe holes provided at 311 mm intervals along the flame. Samples of furnace gas were taken from the flame at these probe holes, and the flame temperature was measured using a suction pyrometer. Extreme care was was taken to ensure that the flame conditions were absolutely stable before gas sampling and temperature measurement began.

It is not proposed to offer any greater details of the experimental work here because the techniques are well established and are described at length elsewhere (Leesley, 1967; Beer and Thring, 1961). The probes used were of a design developed by the International Flame Research Foundation (Hinje and Van der Zijven, 1949).

A total of twenty successful runs was achieved, of which seven were repeats done to confirm high repeatability of the experimental results.

ANALYSIS OF RESULTS

Computation of Combustion Rate Data

A typical burning curve is shown in Figure 5. The fraction of unburnt coal remaining at any point in the flame was calculated from the amount of carbon dioxide present at that point. The time for the flame to travel between two sampling ports was calculated from the volumetric furnace gas flow rate, the average temperature between two points and the cross-sectional area of the furnace.

Rather than use the tedious and inaccurate method of measuring gradients of the burning away curve to find the combustion rate at each sampling port, it was decided to fit an equation to the burning away curve and differentiate.

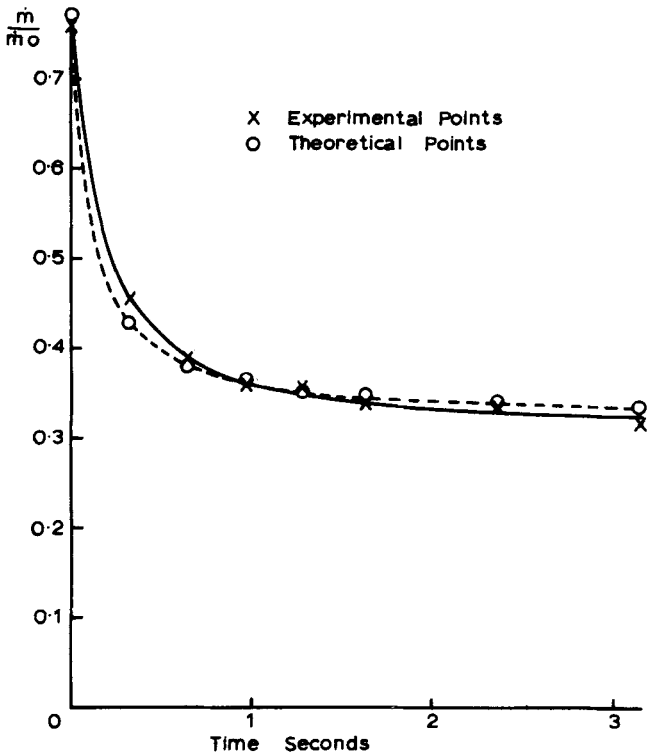

Fig. 5. Comparison of experimental and theoretical burning away curves for coal No. 10.

TABLE 2. PRELIMINARY MULTIPLE CORRELATION RESULTS

Regression equation	Data used	k	n_1	E	r_c
(30)	ALL	8.00×10^5	1.257	17 764	0.953
(31)	ALL	8.47×10^6	1.412	20 200	0.913
(30)	P.D.*	1.69×10^6	1.291	18 820	0.972
(30)	M.D.*	8.10×10^5	0.947	20 520	0.971
(31)	P.D.*	2.51×10^7	1.368	17 858	0.921
(31)	M.D.*	6.14×10^8	1.485	24 760	0.881

* P.D. = Date compiled from polydisperse flames. M.D. = Date compiled from monodisperse flames.

The type of regression equation used was

$$\frac{\dot{m}}{\dot{m}_o} = a + \frac{b}{t + c} \tag{29}$$

where a, b, and c were constants determined for each run. One such theoretically predicted curve is shown plotted alongside the corresponding experimental curve in Figure 5.

Analysis using Traditional Theory

It is relevant to describe first the author's experience in attempting to fit the experimental results to traditional theory (Beer and Thring, 1961) which suggests that the relationships between reaction rate and flame parameters are of the form of Equations (23) and (24), where Equation (23) assumes the combustion to be chemically controlled and Equation (24) assumes diffusion control. In order to find the values of the constants, a series of multiple correlation analyses was performed with the experimental data.

The following two equations were used as a basis for the correlations:

$$\frac{\rho d_o}{6}\left(\frac{m}{m_o}\right)^{-2/3}\frac{d}{dt}\left(\frac{m}{m_o}\right) = \frac{-k}{T^{1/2}}\,p_{O_2}{}^{n_1}\exp\left(\frac{-E}{R_g T}\right) \tag{30}$$

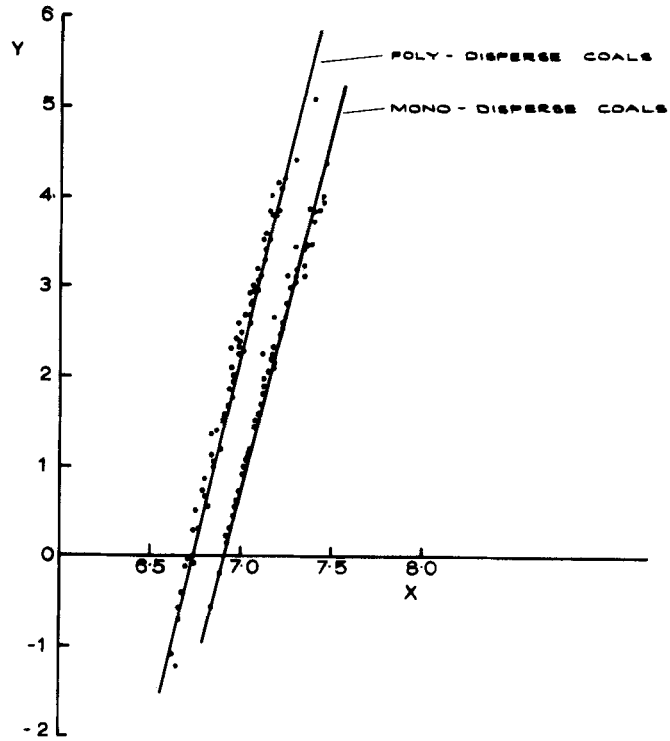

Fig. 6. Regression curve on

$$\frac{\rho do}{6}\left(\frac{m}{m_o}\right)^{-2/3}\frac{d}{dt}\left(\frac{m}{m_o}\right) = \frac{-k}{T^{1/2}}\,p_{O_2}{}^{n_1}\exp\left(\frac{E}{R_g T}\right)$$

$$Y = \mathrm{Log}_e\left\{-\frac{\rho do}{6}\left(\frac{m}{m_o}\right)^{-2/3}\frac{T^{1/2}}{p_{O_2}{}^{n_1}}\frac{d}{dt}\left(\frac{m}{m_o}\right)\right\}$$

$$X = \frac{1}{T} \times 10^4.$$

$$\frac{\rho d_o{}^2}{6}\left(\frac{m}{m_o}\right)^{-1/3}\frac{d}{dt}\left(\frac{m}{m_o}\right) = \frac{-k}{T^{1/2}}\,p_{O_2}{}^{n_1}\exp\left(\frac{-E}{R_g T}\right) \tag{31}$$

The forms of the functions were suggested by an earlier literature survey (Hedley and Leesley, 1965), but, generally, Equation (30) assumes chemical control and Equation (31) assumes diffusion control. The results of the correlation analyses are expressed in two ways: first in Table 2, where the values of the constants and the correlation coefficients are tabulated for each equation, and, second, the graph shown in Figure 6, which is drawn for Equation (30) only. It can be seen from the typical graph that the data collected on runs using monodisperse flames fall on a different line from those of runs using polydisperse flames.

To account for this discrepancy, the theory of dust cloud combustion was extended as described earlier in such a way that Equations (30) and (31) were rewritten as Equations (33) and (34). Thus, we introduce k_1 and k_2 as constants to replace those suggested by traditional theory in Equations (30) and (31).

RESULTS ANALYSIS USING EXTENDED THEORY

In order to assess the value of the new form of Equations (33) and (34), it was necessary to evaluate the constants k_1 and k_2. This was done by plotting $F(Y)$, as defined in Equation (27), against $(\dot{m}/\dot{m}_o)$ for the coals defined in Table 1 on log-log paper. Equations (19) and

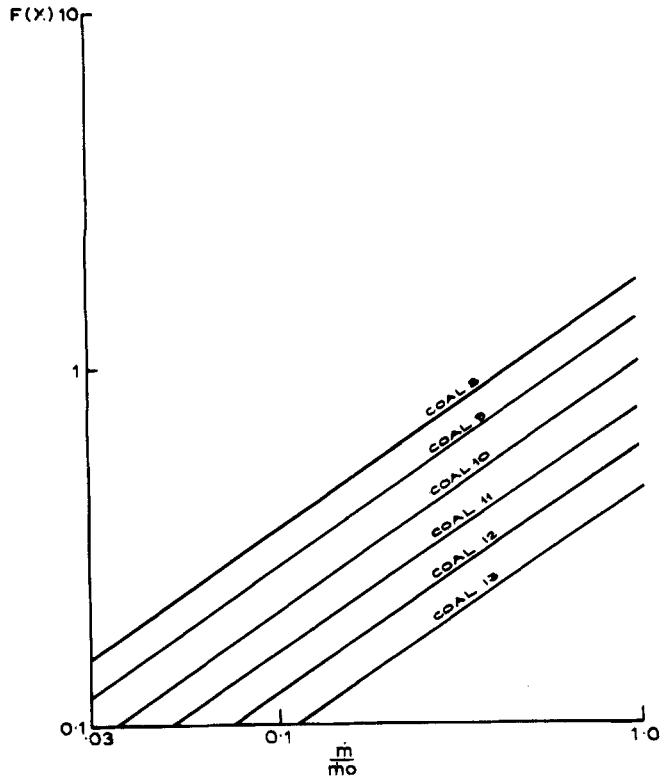

Fig. 7. Graph showing $F(Y)$ plotted against m/m_o for monodisperse coals assuming chemical control.

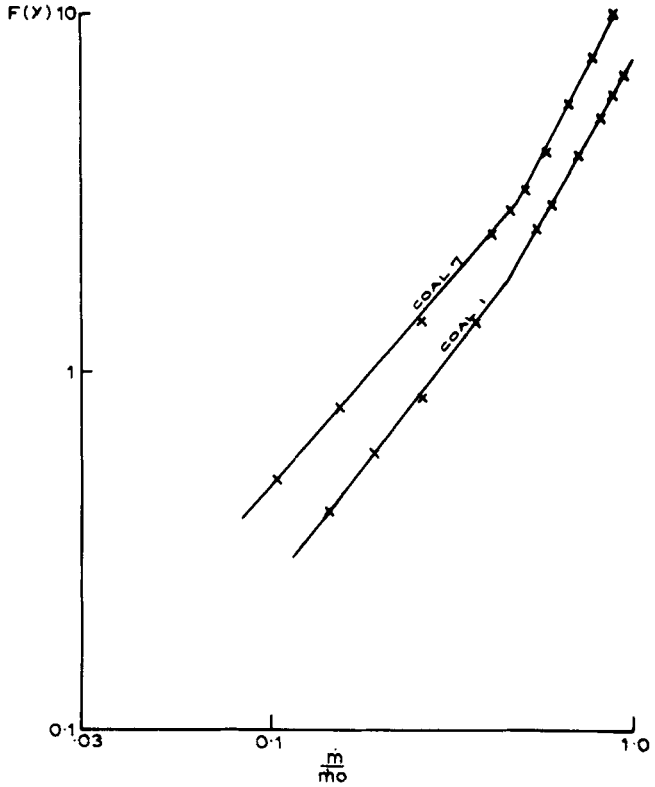

Fig. 8. Graph showing $F(Y)$ plotted against m/m_o for polydisperse coals assuming chemical control.

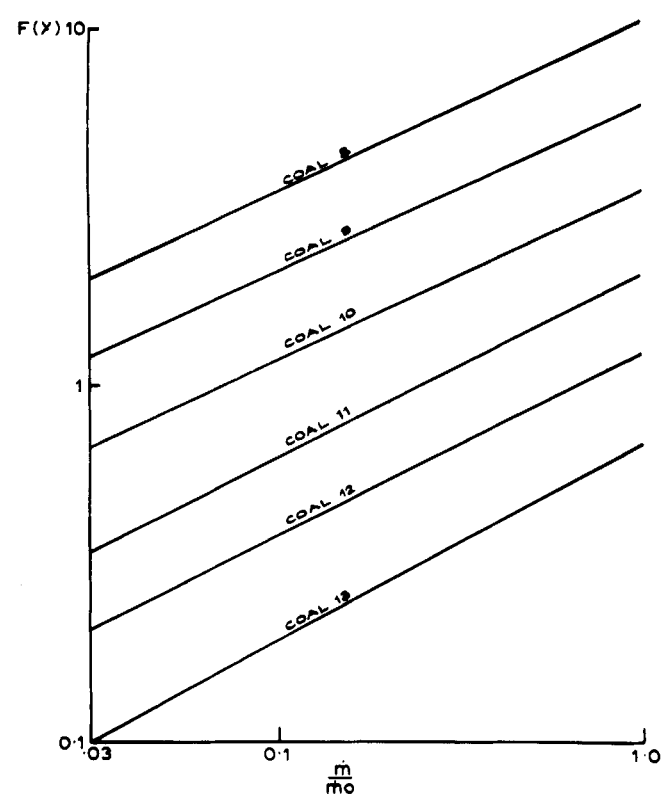

Fig. 9. Graph showing $F(Y)$ plotted against m/m_o for monodisperse coals assuming diffusion control.

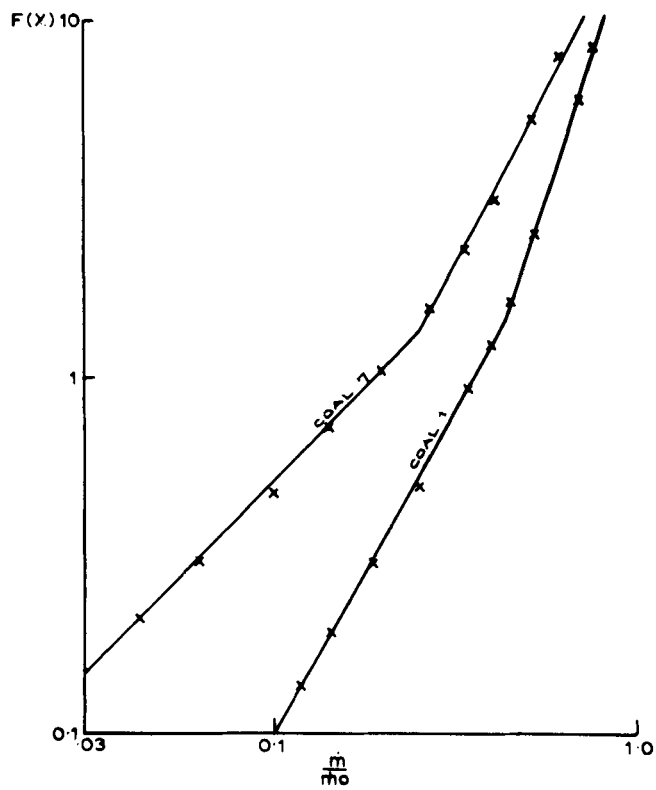

Fig. 10. Graph showing $F(Y)$ plotted against m/m_o for polydisperse coals assuming diffusion control.

(27) were numerically integrated for increasing values of Y which is the dimensionless initial size of a particle which would have just burned away if present. Y is best thought of as a flame length parameter. The lower limit of integration Z must be chosen so as to include all initial diameters of particles which have not burned away after time t; that is

$$Z = X_1 \quad \text{if} \quad Y \leq X_1$$

and

$$Z = Y \quad \text{if} \quad Y > X_1$$

The values of $F(Y)$ were determined numerically by the following series of steps.

Table 3. Values of k_1 and k_2 Showing Value of m/m_o at Point of Changeover for the Polydisperse Coals

Chemical control

Coal No.	k_1	k_2	$\dot{m}/\dot{m}_o$ at change	k_1	k_2
1	7.177	1.889	0.45	4.684	1.277
2	8.356	2.092	0.49	4.646	1.269
3	8.433	2.087	0.49	4.620	1.251
4	8.561	2.060	0.48	4.593	1.213
5	9.306	2.061	0.47	4.615	1.137
6	9.996	2.005	0.53	6.079	1.212
7	11.290	1.951	0.54	7.334	1.248
8	1.711	0.674			
9	1.323	0.674			
10	1.043	0.673			
11	0.767	0.672			
12	0.592	0.672			
13	0.443	0.677			

Diffusion control:

Coal No.	k_1	k_2	$\dot{m}/\dot{m}_o$ at change	k_1	k_2
1	31.41	4.277	0.56	8.517	2.054
2	41.22	4.750	0.56	8.795	2.062
3	43.24	4.849	0.56	8.557	2.019
4	46.82	4.763	0.55	9.265	2.020
5	47.79	4.491	0.54	9.098	1.818
6	57.43	4.598	0.56	10.551	1.715
7	73.82	4.748	0.58	13.962	1.662
8	0.986	0.354			
9	0.586	0.353			
10	0.341	0.359			
11	0.193	0.349			
12	0.117	0.353			
13	0.066	0.365			

Table 4. Results of Final Multiple Correlation Analyses (All Data Used in Each Equation)

Regression equation	k	n_1	E	r_c
(33)	6.34×10^7	0.887	29 230	0.988
(34)	3.15×10^9	0.817	23 600	0.166

The numerical integrations were carried out using Simpsons rule with a step length of $(X_2 - X_1)/200$.

An initial value of $Y = 0.002$ was chosen and the integration performed with the lower limits of integration set to $Z = X_1$ when $X_1 > 0.002$ and $Z = 0.002$ when $X_1 \leq 0.002$.

The whole procedure was repeated with Y increasing in steps of 0.002 up to X_2, that is, until all particles had burnt away and $(\dot{m}/\dot{m}_o)$ became zero.

It can be seen that if Equation (28) is rewritten in the form

$$\log[F(Y)] = \log k_1 + k_2 \log\left(\frac{\dot{m}}{\dot{m}_o}\right) \qquad (32)$$

then a graph of log $[F(Y)]$ plotted against log $(\dot{m}/\dot{m}_o)$ gives an intercept of log k_1 and a slope of k_2. This method was used to calculate k_1 and k_2 for the thirteen coals. The graphs are shown plotted in Figure 7 for the monodisperse fractions assuming chemical control, Figure 8 for polydisperse fractions assuming chemical control, Figure 9 for monodisperse fractions assuming diffusion control, and Figure 10 for polydisperse fractions assuming diffusion

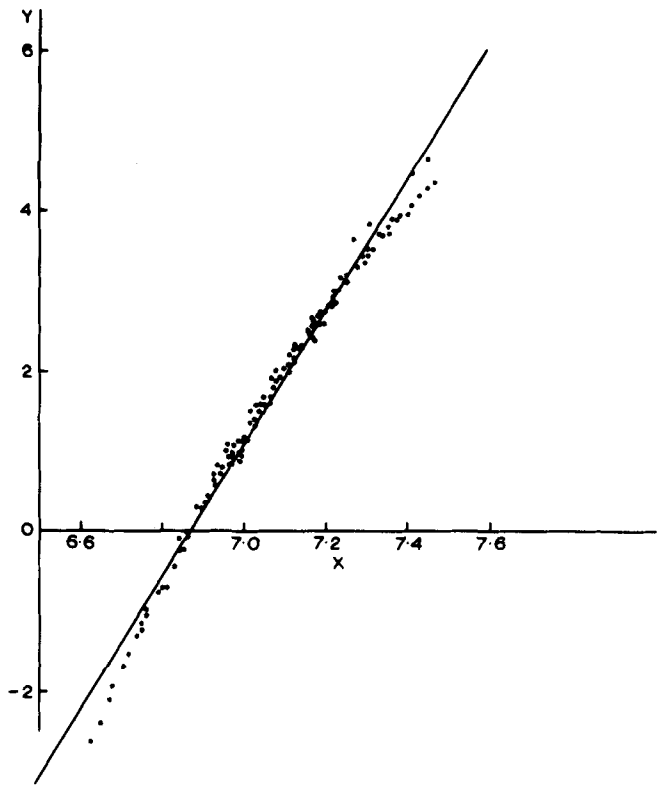

Fig. 11. Regression curve on

$$\frac{\pi\rho\bar{\chi}_i}{2k_1}\left(\frac{\dot{m}}{m_o}\right)^{-k_2}\frac{d}{dt}\left(\frac{\dot{m}}{m_o}\right) = \frac{-k}{T^{1/2}}p_{O_2}{}^{n_1}\exp\left(\frac{-E}{RgT}\right)$$

$$Y = \mathrm{Log}_e\left\{-\frac{\pi\rho\bar{\chi}_i}{2k_1}\left(\frac{\dot{m}}{m_o}\right)^{-k_2}\frac{T^{1/2}}{p_{O_2}{}^{n_1}}\frac{d}{dt}\left(\frac{\dot{m}}{m_o}\right)\right\}$$

$$X = \frac{1}{T} \times 10^4.$$

control. For reasons of clarity, coals 2 to 6 inclusive are omitted from Figures 8 and 10. The slopes (k_2) for monodisperse fractions were found to be approximately equal to 2/3 and 1/3, that is, the values derived for Equations (23) and (24) by Beér. Thus, the method used for calculating k_2 agrees with Beér's theory for the combustion of an almost uniformly sized dust cloud. Values of k_1 and k_2 are given for all coals in Table 3. It can be seen in Figures 8 and 10 that the plotting of log $[F(Y)]$ against log $(\dot{m}/\dot{m}_o)$ for polydisperse fractions does not give a straight line. However, each curve can be approximated by two straight lines, thus giving two different values of both k_1 and k_2 for the early and late parts of the flame. The point of changeover given in Table 3 has no physical significance and is merely a convenient point for expressing the position of the change in slope. Using the calculated values of k_1 and k_2, the multiple correlation analyses were repeated using the following equations:

$$\frac{\pi\rho\bar{x}_i}{2k_1}\left(\frac{\dot{m}}{\dot{m}_o}\right)^{-k_2}\frac{d}{dt}\left(\frac{\dot{m}}{\dot{m}_o}\right) = \frac{-k}{T^{1/2}}p_{O_2}{}^{n_1}\exp\left(\frac{-E}{R_gT}\right) \qquad (33)$$

$$\frac{\pi\rho\bar{x}_i{}^2}{2k_1}\left(\frac{\dot{m}}{\dot{m}_o}\right)^{-k_2}\frac{d}{dt}\left(\frac{\dot{m}}{\dot{m}_o}\right) = \frac{-k}{T^{1/2}}p_{O_2}{}^{n_1}\exp\left(\frac{-E}{R_gT}\right) \qquad (34)$$

where Equation (33) uses the values of k_1 and k_2 calcu-

lated assuming chemical control and Equation (34) had values of k_1 and k_2 calculated assuming diffusion control. Once again, the results of the correlation analyses are shown in two ways, first in Table 4 and second in graphical form for Equation (33) only. This time the data compiled for both polydisperse and monodisperse clouds all fall on one straight line.

Discussion of the Results of the Correlation Analyses

A comparison of the graph plotted using traditional theory in Figure 6 with that using extended theory in Figure 11 shows that equations predicted by the extended theory can be fitted to all the experimental data using the one value each of the constants k, n_1, and E. To save space, only Equation (33) is plotted.

The results are better fitted to equations derived assuming chemical control. This suggests that in the temperature range (700° to 1 400°C) and the size range (0 to 200 μ) chosen, the combustion rate of pulverized anthracite is controlled by the rate of chemical reaction at the particle surface. Moreover, the theoretical equation giving the best fit to the experimental results is

$$\frac{\rho\pi\overline{x_i}}{2k_1}\left(\frac{\dot{m}}{\dot{m}_o}\right)^{-k_2}\frac{d}{dt}\left(\frac{\dot{m}}{\dot{m}_o}\right) = \frac{-6.34\times10^7}{T^{1/2}}\,p_{O_2}{}^{0.887}\exp\left(\frac{-29\,230}{R_gT}\right) \tag{35}$$

which gave a correlation coefficient of 0.9875.

In order of the reaction n_1 in Equation (35) is 0.887. This agrees very well with those workers (Hedley and Leesley, 1965) who have suggested that the value of n_1 should lie between zero and unity. Marsden (1964) and Guldenpfennig (1964) have found values of n_1 greater than unity burning anthracite in conditions similar to those used in these trials. However, their results were fitted to equations derived using the old theory, where k_2 is assumed to be 2/3 for polydisperse clouds. It is likely that forcing the experimental results into a spurious regression equation may have affected the value of n_1 and caused it to take a high value. The constant E which is generally called the apparent activation energy of the reaction takes a value of 29 230 cal/mole in Equation (35). This agrees satisfactorily with the value of 19 610 found by Marsden (1964).

Wicke suggests that E may be different in different temperature ranges. No evidence of a change in E was found in the temperature range 700° to 1 400°C, although there is some evidence of a change in slope towards the extremes of the temperature range in Figure 11.

Predicting the Combustion Rate from Initial Particle Size Distribution Parameters b and n

The constants b and n for a fuel may be measured by performing a sieve analysis on a carefully drawn sample of the fuel as described by Rosin and Rammler (1933). Numerical integration of Equations (19) and (27) with a step length of $(X_1 - X_2)/200$ will give k_1 and k_2. Note that for a polydisperse coal (the normal industrial case), the values may change approximately halfway along the flame as shown in Figure 8. Fitting the constants for the two portions of the flame into Equation (35) will give a combustion rate relationship which for Welsh anthracite gave an extremely close fit to experimentally measured values. For fuels which contain high volatile matter, Equation (35) is likely to be of no value in the initial stages of the flame while volatiles are being evolved with the corresponding dramatic changes in size. However, as soon as the fuel is reduced to a char, or coke, Equation (35) should apply.

NOTATION

a, b, c = constants
D = diameter of single particle, m
d_o = mean diameter of particle in a sized fraction before combustion begins, m
E = activation energy, cal/mole
F = function defined by Equation (27)
f, f_C, f_D = functions
k, k_C, k_D = constants
k_1, k_2, k' = constants, $k' = -k/\pi$
m = mass of single particle, g
$\dot{m}$ = mass flow rate, g/s
$\dot{m}_o$ = initial mass flow rate, g/s
n, n_1, n_2 = constants
P = $-\exp(-\gamma X_1{}^n) - \exp(-\gamma X_2{}^n)$
p_{O_2} = partial oxygen pressure, mbar
q = constant
R_g = gas constant
r_c = correlation coefficient
T = temperature, °C
t = time, s
W = weight fraction remaining on a given sieve size
X, X_1, X_2 = dimensionless particle sizes
x, x_1, x_2 = particle sizes, m
$\overline{x_i}$ = characteristic particle size, m
y = particle size, m
y_o = particle size parameter, m
Y = dimensionless particle size parameter
Z = integration limit, dimensionless particle size
z = particle size, m
β = constant
γ = constant defined by Equation (14)
ρ = coal density, g/m^3
θ = a function

LITERATURE CITED

Leesley, M. E., "A Study of the Effect of Particle Size on the Combustion Rate of an Anthracite Dust Cloud," Ph.D. thesis, Univ. Sheffield, England (1967).

Beer, J. M., and M. W. Thring, "Some Measurements of the Rate of Combustion of Pulverized Anthracite in a Controlled Mixing One-Dimensional Furnace," Proc. Anthr. Coal, Bull., 1975, Mineral Industries Exprl. Station, Penn. State Univ., (Sept., 1961).

Rosin, P. O., and E. J. Rammler, "The Laws Governing the Fineness of Powered Coal," *J. Inst. Fuel*, 7, 29 (Oct., 1933).

Leesley, M. E., and R. G. Siddall, "The Combustion Rate of a Pulverized Anthracite Dustcloud of known Initial Size," *ibid.*, 42, 169 (Mar., 1972).

Leesley, M. E., and A. B. Hedley, "The Effects of Particle Size Distribution on the Combustion Rate of an Anthracite Dustcloud," *ibid.*, 224 (Apr., 1972).

Hedley, A. B., and M. E. Leesley, "Burning characteristics of Pulverized Coal," *ibid.*, 38, 492 (Nov., 1965).

Hinje, J. O., and G. B. Van der Zijuen, "Transfer of heat and matter in the Turbulent Mixing Zone of an Axially Symmetrical Jet," *Appl. Sci. Res. Hague AL*, 435 (1949).

Marsden, C., "Anthracite Dustcloud Combustion," Ph.D. thesis, Univ. Sheffield, England (1964).

Guldenpfennig, F. W., "A Study of the Effect of Pressure on the Combustion Rate of an Anthracite Dustcloud," Ph.D. thesis, Univ. Sheffield, England (1964).

Beer, J. M., and K. B. Lee, "The Effect of the Residence Time Distribution on the Performance and Efficiency of Combustion," Tenth Symp. on Comb., p. 1187.

Wicke, E., "Contributions to the Combustion Mechanism of Carbon," Fifth Symp. on Comb., p. 245.

Manuscript received August 3, 1976; revision received March 14 and accepted May 3, 1977.